

Energy feedback and synchronous dynamics of Hindmarsh-Rose neuron model with memristor

K Usha, P A Subha

Citation: Chin. Phys. B . 2019, 28(2): 020502. **doi:** 10.1088/1674-1056/28/2/020502
Journal homepage: http://cpb.iphy.ac.cn; http://iopscience.iop.org/cpb

What follows is a list of articles you may be interested in

A generalized model of TiO_x-based memristive devices andits application for image processing

Jiangwei Zhang(张江伟), Zhensen Tang(汤振森), Nuo Xu(许诺), Yao Wang(王耀), Honghui Sun(孙红辉), Zhiyuan Wang(王之元), Liang Fang(方粮)

Chin. Phys. B . 2017, 26(9): 090502. **doi:** 10.1088/1674-1056/26/9/090502

Attempt to generalize fractional-order electric elements to complex-order ones

Gangquan Si(司刚全), Lijie Diao(刁利杰), Jianwei Zhu(朱建伟), Yuhang Lei(雷好航), Yanbin Zhang(张彦斌)

Chin. Phys. B . 2017, 26(6): 060503. **doi:** 10.1088/1674-1056/26/6/060503

Dynamical characteristics of an HP memristor based on an equivalent circuit model in a chaotic oscillator

Yuan Fang, Wang Guang-Yi, Wang Xiao-Yuan

Chin. Phys. B . 2015, 24(6): 060506. **doi:** 10.1088/1674-1056/24/6/060506

Mapping equivalent approach to analysis and realization of memristor-based dynamical circuit

Bao Bo-Cheng, Hu Feng-Wei, Liu Zhong, Xu Jian-Ping

Chin. Phys. B . 2014, 23(7): 070503. **doi:** 10.1088/1674-1056/23/7/070503

Exponential synchronization of coupled memristive neural networks via pinning control

Wang Guan, Shen Yi, Yin Quan

Chin. Phys. B . 2013, 22(5): 050504. **doi:** 10.1088/1674-1056/22/5/050504

Energy feedback and synchronous dynamics of Hindmarsh–Rose neuron model with memristor

K Usha[1] and P A Subha[2,†]

[1] *Department of physics, University of Calicut, Kerala 673635, India*

[2] *Department of physics, Farook College, University of Calicut, Kerala 673632, India*

(Received 2 October 2018; revised manuscript received 19 November 2018; published online 10 January 2019)

We analyze the energy aspects of single and coupled Hindmarsh–Rose (HR) neuron models with a quadratic flux controlled memristor. The energy function for HR neuron with memristor has been derived and the dynamics have been analyzed in the presence of various external stimuli. We found that the bursting mode of the system changes with external forcing. The negative feedback in Hamilton energy function effectively stabilizes the chaotic trajectories and controls the phase space. The Lyapunov exponents have been plotted to verify the stabilization of trajectories. The energy aspects during the synchronous dynamics of electrically coupled neurons have been analyzed. As the coupling strength increases, the average energy fluctuates and stabilizes at the point of synchronization. When the neurons are coupled via chemical synapse, the average energy variations show three important regimes: a fluctuating regime corresponding to the desynchronized, a stable region indicating synchronized and a linearly increasing regime corresponding to the amplitude death states have been observed. The synchronization transitions are verified by plotting the transverse Lyapunov exponents. The proposed method has a large number of applications in controlling coupled chaotic systems and in analyzing the energy change during various metabolic processes.

Keywords: HR model, memristor, Hamilton energy, energy feedback, synchronization

PACS: 05.45.–a **DOI:** 10.1088/1674-1056/28/2/020502

1. Introduction

The transmission of nerve impulses in the brain occurs via the propagation of action potentials and a large fraction of the total energy consumed by brain is utilized to generate the firing patterns. The evaluation of required metabolic energy to maintain the signaling activity in neurons is an active research area.[1] The collective dynamics of neural networks have a considerable influence in the propagation of information from one region to another and their collective behavior can be greatly influenced by the energy demands. Neuron models are used to analyze the connection between energy demands and firing modes.[2] The Hamilton energy associated with the dynamical system can be derived using the generalized Hamiltonian approach.[3] Using this formalism, Sarasola *et al.* have derived the energy function associated with Lorenz, Rossler, and Chua systems.[4] Moujahid *et al.* have reported the energy consumption during the synchronization process in electrically coupled HR neurons.[5] The consumption of energy in transmitting nerve impulse using Hodgkin–Huxley model has also been reported.[6]

It is important to investigate the energy utilization of neurons subjected to different kinds of external force during information encoding. Biological experiments confirm that the electrical activities of neurons change by adjusting extracellular calcium or potassium concentrations.[7] The Hindmarsh–Rose (HR) neuron oscillates periodically for small and large external current, whereas for intermediate currents they become chaotic.[8] The periodic external forcing also influences the bursting modes and neuronal activities.[9] In addition, computational models have been developed to study the effect of noise.[10–12] The statistical features of Gaussian white noise seem to be appropriate to mimic the complex behavior shown by a neuron under the influence of other neurons and the environment. Zambrano *et al.* have analyzed the synchronization of uncoupled FitzHugh–Nagumo neurons with common noise both experimentally and numerically.[13] Noise-induced resonances in the HR model has also been studied.[14] Wang *et al.* have reported that, the forced HR neurons with white Gaussian noise leads to firing modes like multi-modal firing, intrinsic oscillation, and bi-modal firing.[15] Lindner *et al.* have studied the dynamics of mathematical models of excitable systems in the presence of white Gaussian noise.[16]

Recent studies confirm that a two terminal electric device called memristor can mimic the the key characteristics of synapses and neurons. A memristor models the effect of electromagnetic field created as a result of the exchange of ions across the nerve membrane. The electrical activities in the cardiac tissues exposed to electromagnetic radiation can be described using memristor models. This provides significant clues about the mechanism of heart disorders induced by electromagnetic radiation.[17] The synchronization of coupled memristive neural network via pinning control has been proposed by Guan *et al.*[18] Recently Ma *et al.* have discussed the RCL-shunted junction circuit with memristor.[19] The control of dynamical systems with negative feedback in energy has

†Corresponding author. E-mail: pasubha@farookcollege.ac.in

© 2019 Chinese Physical Society and IOP Publishing Ltd

recently been reported.[20]

In this paper, we analyze the energy aspects of single and coupled HR neuron model with a memristor. The HR neuron model with quadratic flux controlled memristor is presented in Section 2. The Hamilton energy of the system is derived in Section 3 and the energy change in the presence of different external stimuli has been discussed. In addition, the control of chaotic trajectories by applying a negative feedback is discussed in this section. The energy aspects during the synchronization process of electrically and chemically coupled HR neurons are studied in Section 4. Finally, Section 5 concludes the study.

2. Model

The continuous exchange of charged ions across the nerve membrane induce an electromagnetic field that controls the membrane potential of neurons. Recently Ma *et al.* proposed that memristors can be used to bridge the magnetic flux and membrane potential. This coupling influences signal transmission via the superposition of electric field.[9,21] Memristors are used to realize the coupling. The HR model with memristor is capable of producing biologically relevant dynamical states such as anti-phase oscillations, co-existence of resting and spiking state *etc*.[22] The dynamical equations of HR neuron model with quadratic flux controlled memristor have the form:[9]

$$\dot{x} = y + ax^2 - x^3 - z + I - k_1\rho(\phi)x,$$
$$\dot{y} = 1 - bx^2 - y,\ \ \dot{z} = r(R(x - x_e) - z),\ \ \dot{\phi} = k_2 x - k_3\phi, \quad (1)$$

where $\rho(\phi) = \alpha\phi^2 + \beta\phi + \gamma$. The membrane potential of the neuron is represented using the variable x. y denotes the recovery variable representing the rate of change of fast current of K^+ or Na^+ ions and z denotes the adaptation variable that capture the slower dynamics of other ion channels. The parameters a and b denote activation and inactivation of the fast ion channel. R and x_e describe activation and inactivation of the slow ion channel. The speed of variation of z is controlled by r.[23–25] The parameter I represents the external stimuli.[26,27] The fourth variable ϕ denotes magnetic flux across the nerve membrane. A memristor with memductance $\rho(\phi) = \mathrm{d}q(\phi)/\mathrm{d}\phi$ is used to realize the coupling between magnetic flux of the field and membrane potential. It is possible to model $\rho(\phi)$ using a quadratic term. The memductance after suitable scaling is taken as $\rho(\phi) = \alpha\phi^2 + \beta\phi + \gamma$, α, β, and γ are parameters.[28] The term $k_1\rho(\phi)x$ denotes the induced current through electromagnetic induction, where k_1 represents the modulation intensity of electromagnetic field. Relation between induced current and flux change can be understood using Faraday's law of electromagnetic induction.[29] The term k_2x represents the change in magnetic flux induced by membrane potential of the cell and $k_3\phi$ denotes the leakage of magnetic flux. The parameters used are $a = 3.0$, $b = 5.0$, $R = 4.0$, $r = 0.006$, $I = 3.1$, and $x_e = -1.61$.[30]

We have analyzed the dynamics of the system in Eq. (1) by varying the external current I. The fourth order Runge–Kutta algorithm is applied for numerical calculations. The memristor parameters are taken as $\beta = 1.0$, $\gamma = 1.0$, $k_2 = 0.9$, and $k_3 = 0.5$. The value of k_1 is fixed at 0.1 and by increasing the value of α the inter spike interval bifurcation (*ISI*) diagrams have been plotted. Figures 1(a), 1(b), and 1(c) show the distribution of *ISI* for $\alpha = 0.1$, 0.4, and 0.8 respectively. It is found that as the value of α is increased, the system eventually transforms to its normal response state. The study has been extended by fixing $\alpha = 0.1$ and by varying k_1. Figures 1(d), 1(e), and 1(f) represent the *I versus ISI* for $k_1 = 0.8$, 0.4, and 0.1 respectively. From the plots it is clear that, for constant α, a decrease in k_1 is needed for normal firing. The response of a neuron with electromagnetic induction described by quadratic flux controlled memristor to external signals can be enhanced by properly selecting the memristor parameters.[21]

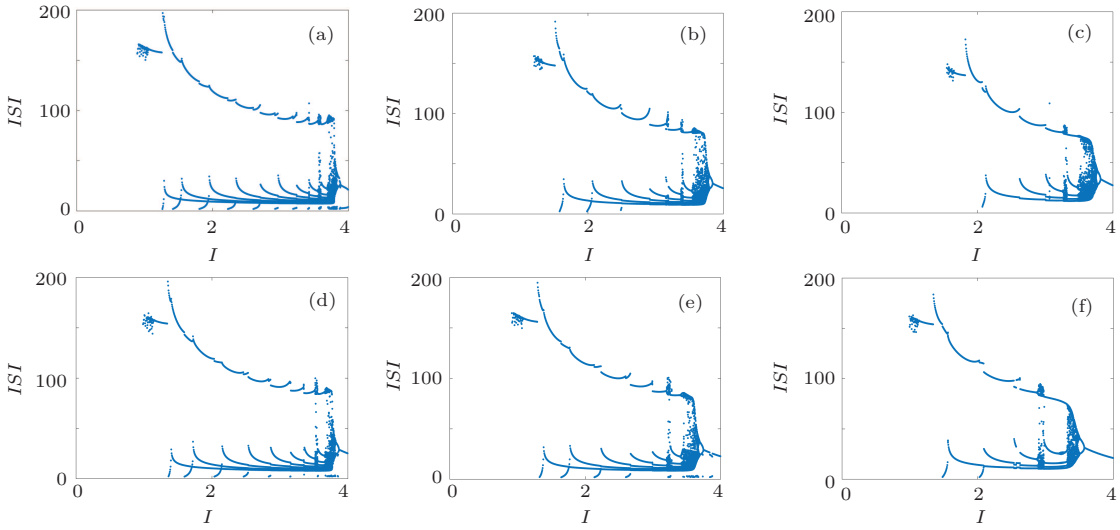


Fig. 1. The *ISI* bifurcation diagram of HR neuron with memristor. Figures 1(a), 1(b), and 1(c) shows *I versus ISI* for $k_1 = 0.1$ and $\alpha = 0.1$, 0.4, and 0.8. Figures 1(d), 1(e), and 1(f) are drawn for $\alpha = 0.1$, $k_1 = 0.8$, 0.4, and 0.1. The parameters β and γ are set as 1.0.

3. Energy aspects

In this section, we derive the Hamilton energy of HR model with quadratic flux controlled memristor. The differential equation of an autonomous dynamical system is of the form: $\dot{x} = f(x)$. According to Helmholtz's theorem the velocity vector field $f(x)$ can be written as:

$$f(x) = f_{\mathrm{c}}(x) + f_{\mathrm{d}}(x), \tag{2}$$

where f_{c} component of the vector field is conservative. This does not contribute to the energy change along any trajectory of the system and satisfies the following equation,

$$\nabla H^{\mathrm{T}} f_{\mathrm{c}}(x) = 0. \tag{3}$$

The function $H(x)$ is the generalized Hamiltonian for the conservative system as long as it can be rewritten in the form $\dot{x} = J(x)\nabla H$, where J is a skew symmetric matrix that satisfies Jacobi's closure condition.[31] The component f_{d} is composed of velocity-dependent terms and contribute to the divergence.[9] The dissipation of energy due to the f_{d} part obeys the relation:

$$\nabla H^{\mathrm{T}} f_{\mathrm{d}}(x) = \dot{H}. \tag{4}$$

The conservative and dissipative part of HR model in Eq. (1) can be expressed in the form:

$$\begin{bmatrix} \dot{x} \\ \dot{y} \\ \dot{z} \\ \dot{\phi} \end{bmatrix} = f_{\mathrm{c}}(x,y,z,\phi) + f_{\mathrm{d}}(x,y,z,\phi),$$

where

$$f_{\mathrm{c}}(x,y,z,\phi) = \begin{bmatrix} y - z + I - \phi \\ 1 - bx^2 \\ rR(x - x_{\mathrm{e}}) \\ k_2 x \end{bmatrix}$$

and

$$f_{\mathrm{d}}(x,y,z,\phi) = \begin{bmatrix} ax^2 - x^3 - k_1\rho(\phi)x + \phi \\ -y \\ -rz \\ -k_3\phi \end{bmatrix}.$$

Then, according to Eq. (3), the Hamilton energy associated with the system will satisfy the following partial differential equation:

$$(y - z + I - \phi)\frac{\partial H}{\partial x} + (1 - bx^2)\frac{\partial H}{\partial y} + rR(x - x_{\mathrm{e}})\frac{\partial H}{\partial z} + k_2 x\frac{\partial H}{\partial \phi} = 0. \tag{5}$$

A general solution for Eq. (5) is of the form:

$$H = \frac{2}{3}bx^3 - 2x + rR(x - x_{\mathrm{e}})^2 + (y - z + I - \phi)^2 + k_2 x^2. \tag{6}$$

The rate of change of Hamilton energy function is:

$$\dot{H} = 2bx^2\dot{x} - 2\dot{x} + 2rR(x - x_{\mathrm{e}})\dot{x} + 2(y - z + I - \phi)(\dot{y} - \dot{z} - \dot{\phi}) + 2k_2 x\dot{x}. \tag{7}$$

Substituting the values of $\dot{x}$, $\dot{y}$, $\dot{z}$, and $\dot{\phi}$ from Eq. (1), we obtain,

$$\begin{aligned} \dot{H} = {} & 2bx^2(y + ax^2 - x^3 - z + I - k_1\rho(\phi)x) - 2(y + ax^2 - x^3 - z + I - k_1\rho(\phi)x) \\ & + 2rR(x - x_{\mathrm{e}})(y + ax^2 - x^3 - z + I - k_1\rho(\phi)x) \\ & + 2(y - z + I - \phi)(1 - bx^2 - y - rR(x - x_{\mathrm{e}}) + rz - k_2 x + k_3\phi \\ & + 2k_2 x(y + ax^2 - x^3 - z + I - k_1\rho(\phi)x), \end{aligned} \tag{8}$$

rearranging Eq. (8), $\dot{H}$ becomes,

$$\begin{aligned} \dot{H} = {} & 2bx^2(y - z + I_{\mathrm{ext}} - \phi) + 2bx^2(ax^2 - x^3 - k_1\rho(\phi)x + \phi) - 2(y - z + I_{ext} - \phi) - 2(ax^2 - x^3 - k_1\rho(\phi)x + \phi) \\ & + 2rR(x - x_{\mathrm{e}})(y - z + I - \phi) + 2rR(x - x_{\mathrm{e}})(ax^2 - x^3 - k_1\rho(\phi)x + \phi) \\ & + 2(y - z + I_{\mathrm{ext}} - \phi)(1 - bx^2 - y - rR(x - x_{\mathrm{e}}) + rz - k_2 x + k_3\phi) \\ & + 2k_2 x(y - z + I - \phi) + 2k_2 x(ax^2 - x^3 - k_1\rho(\phi)x + \phi), \end{aligned} \tag{9}$$

simplifying and rearranging Eq. (9), the expression for $\dot{H}$ takes the form,

$$\dot{H} = 2(ax^2 - x^3 - k_1\rho(\phi)x + \phi)(bx^2 - 1 + rR(x - x_{\mathrm{e}}) + k_2 x) + 2(y - z + I - \phi)(-y + rz + k_3\phi), \tag{10}$$

and hence obeys the relation in Eq. (4).

The average energy of the system is evaluated using the expression,

$$\langle H \rangle = \int_{t_0}^{t_0+T} H(x,y,z,\phi)\,\mathrm{d}t/T, \tag{11}$$

where T is the energy calculation period (1000 time units) and t_0 is the starting time to calculate the average energy. Figure 2 shows the variations in the average energy with the external forcing current (I). The parameters used are taken as: $a = 3.0$, $b = 5.0$, $R = 4.0$, $r = 0.006$, $x_e = -1.61$, $k_1 = 0.1$, $k_2 = 0.9$, and $k_3 = 0.5$, $\alpha = 0.4$, $\beta = 0.02$, and $\gamma = 0.1$.[9] From the plot it is clear that as I is increased, the average energy decreases.

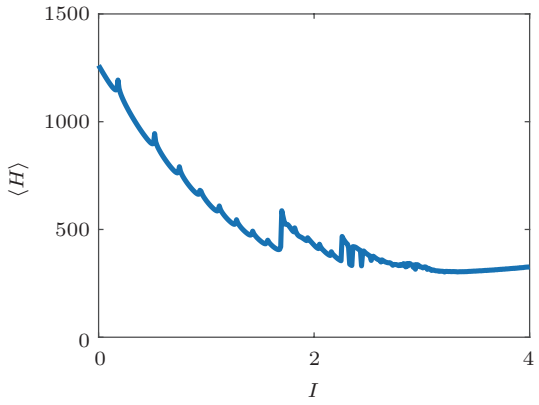


Fig. 2. The variations in average energy of HR neuron with quadratic flux controlled memristor for different values of external current.

We have further analyzed the rate of change of Hamilton energy in the resting and bursting state of membrane potential by applying various external stimuli.

Case 1: Constant external stimulus

A constant external current (I) has been applied to the system. The value of I is changed from 2.0 to 3.0 at $t = 1000$ and then switched to 1.0 at $t = 1500$, as depicted in Fig. 3(a).

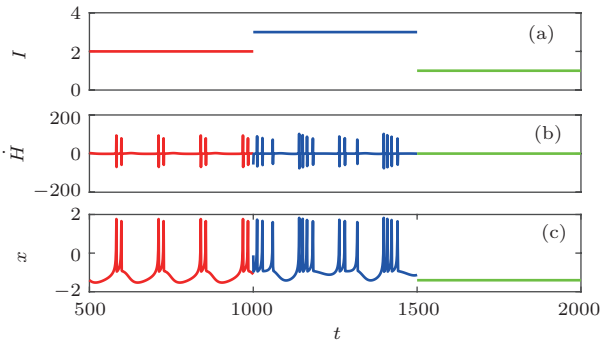


Fig. 3. (a) Variation of external current (b) rate of change of energy function and (c) time evolution of membrane potential of neuron. The external current I is changed from 2.0 to 3.0 at $t = 1000$ time units and switched to 1.0 at $t = 1500$ time units.

The corresponding variations in energy utilization and membrane potential are shown in Figs. 3(b) and 3(c) respectively. From the plots it is clear that as the external current is varied the bursting mode of neuron change and for generating each action potential energy is consumed. The energy demand is a maximum during the repolarization period of the spike and at a minimum during the refractory period between two spikes. The energy utilization approaches zero when the membrane potential is close to the quiescent state.

Case 2: Periodic external stimulus

The effect of periodic stimulus in neural activity has been analyzed by applying an input of the form $I = I_1 + A\sin(0.05t)$, where $I_1 = 3.1$ and A represents the amplitude. The membrane potential and energy utilization during the electrical activities are plotted. The value of A is changed from 0.1 to 1.0 at $t = 1000$ and then switched to 2.0 at $t = 1500$, as shown in Fig. 4(a). In the case of periodic input, A acts as a control parameter for generating different types of electrical responses. As A is increased, the number of spikes per burst in membrane potential is also increased; as shown in Fig. 4(c). The transition in bursting mode induce some transition in Hamilton energy. In the case of state with less number of spikes per burst, the Hamilton energy consumed also become smaller as depicted in Fig. 4(b).

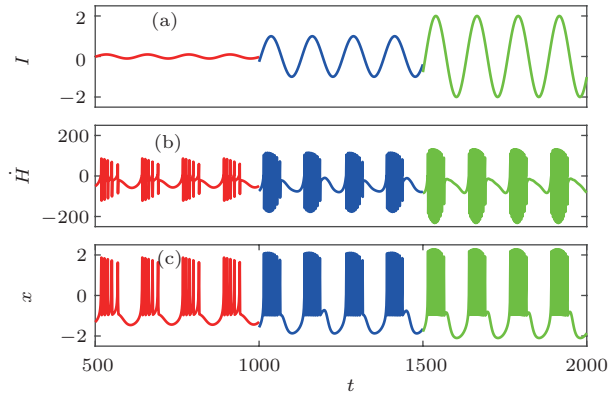


Fig. 4. (a) Variation of periodic input (b) rate of change of energy function and (c) time evolution of membrane potential of neuron. The external periodic forcing has the form $I = I_1 + A\sin(0.05t)$. I_1 is fixed at 3.1 and A is changed from 0.1 to 1.0 at $t = 1000$ and then switched to 2.0 at $t = 1500$.

Case 3: White Gaussian noise

The influence of noise in the firing pattern is discussed in Fig. 5.

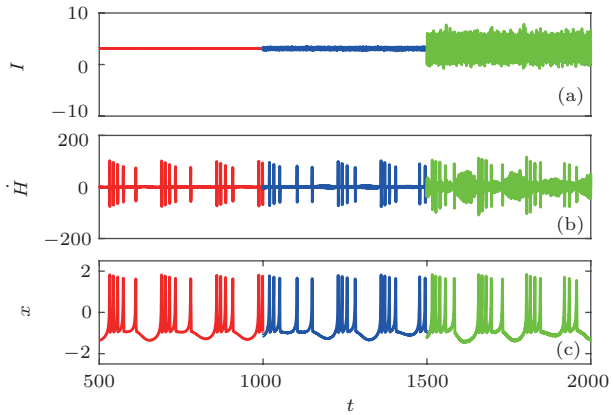


Fig. 5. External noise variations (b) rate of change of energy function and (c) time evolution of membrane potential of neuron. The noise applied is $I = I_1 + \zeta\xi(t)$. $I_1 = 3.1$, ζ is changed from 0.01 to 0.1 at $t = 1000$ and then switched to 1.0 at $t = 1500$.

White Gaussian noise is added through the electrical potential of the membrane; *i.e.*, the effective current imposed to the neuron contains a random term.[32] The noise is of the form $I = I_1 + \zeta\xi(t)$, with parameters $\langle\xi(t)\rangle = 0$, $\langle\xi(t)\,\xi^T(t+\tau)\rangle = \delta(\tau)$ and ζ defines the noise intensity. The value of I_1 is fixed as 3.1 and ζ is changed from 0.01 to 0.1 at $t = 1000$ and then switched to 1.0 at $t = 1500$ as shown in Fig. 5(a). The corresponding variations in membrane potential are shown in Fig. 5(c). From the plot it is clear that the bursting mode changes with the increase in noise intensity. The energy utilization in the presence of noise is depicted in Fig. 5(b). It is confirmed that noisy external stimulus can trigger complex discharge in energy utilization and the effect of noise is more evident in the refractory period of the action potential.

The bifurcation diagrams in (A–$X_{\max}$) and (A–ISI) planes for periodic input are shown in Figs. 6(a) and 6(b) respectively. The amplitude of periodic forcing is varied as $0 \le A \le 4$. The plots show that, an alternate sequence bursting states occur with the increase in A. The bifurcations in the presence of the noisy external forcing are shown in Figs. 6(c) and 6(d). The noise intensity is varied in the range $0 \le \zeta \le 1$. It is found that an increase in ζ produces the complex rhythm and the electrical discharge of the nerve cell becomes more complex leading to chaos.

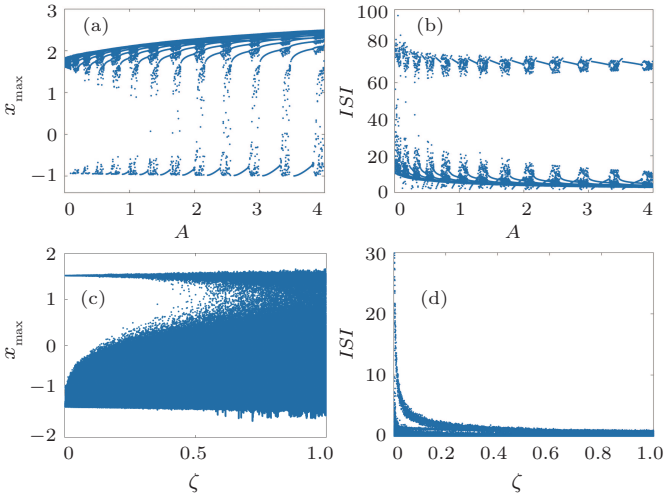


Fig. 6. The bifurcation diagrams. Figures 6(a) and 6(b) show $X_{\max}$ and ISI by varying the amplitude of periodic forcing. Figures 6(c) and 6(d) show $X_{\max}$ and ISI by varying the intensity of external noise.

4. Energy feedback

The Hamilton energy of the system depends on all system parameters, and hence the changes made to energy function causes significant change in the phase space of the dynamic system.[20] The change in energy is realized by giving a negative feedback as follows:

$$\dot{H} = 2(ax^2 - x^3 - k_1\rho(\phi)x + \phi)(bx^2 - 1 + rR(x - x_e) + k_2x) + 2(y - z + I_{ext} - \phi)(-y + rz + k_3\phi) - k_4H, \quad (12)$$

where k_4 is the feedback gain. The phase space dynamics in the (X–H) plane by varying k_4 has been plotted.

Case 1: Constant external stimulus

The formation of attractors in the presence of constant current ($I = 3.1$) is illustrated in Fig. 7. The phase space for $k_4 = 0.0$, $k_4 = 1.0$, $k_4 = 5.0$, $k_4 = 10.0$ are shown in Figs. 7(a), 7(b), 7(c), and 7(d), respectively. As the feedback gain is increased, the number of dense orbits in the attractor is reduced and the chaotic trajectories are controlled. The results are further confirmed by plotting the largest Lyapunov exponent (LLE). The variation of LLE with k_4 is shown in Fig. 8. It is found that the LLE is decreased below zero with increase in k_4 and ensure the stabilization of chaotic trajectories.

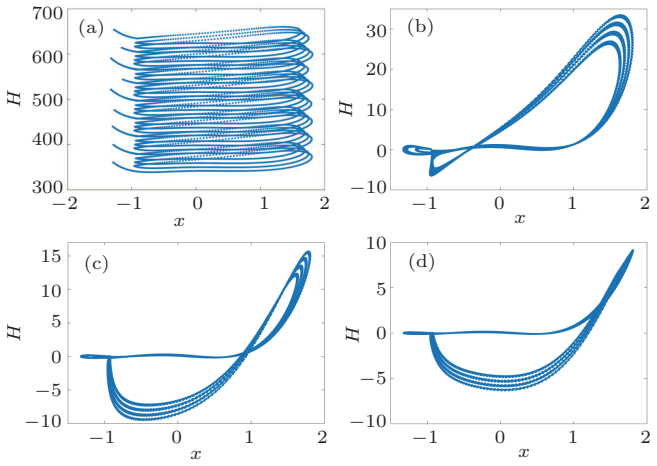


Fig. 7. The phase space of dynamics for $I = 3.1$. The energy feedback obeys Eq. (12). (a) $k_4 = 0$, (b) $k_4 = 1.0$, (c) $k_4 = 5.0$, and (d) $k_4 = 10.0$.

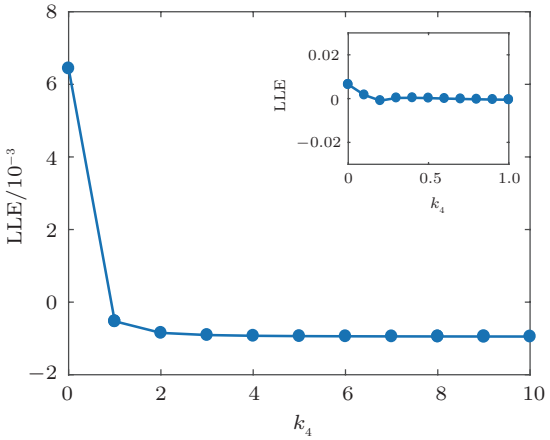


Fig. 8. Transition of LLE for different feedback gains in energy function in the presence of constant external current. The inserted figure is the enlarged version.

Case 2: Periodic external stimulus

The phase space dynamics in the presence periodic input $I = I_1 + 2\sin(0.05t)$ for $k_4 = 0$, $k_4 = 1.0$, $k_4 = 5.0$, and $k_4 = 10.0$ are shown in Figs. 9(a), 9(b), 9(c), and 9(d) respectively.

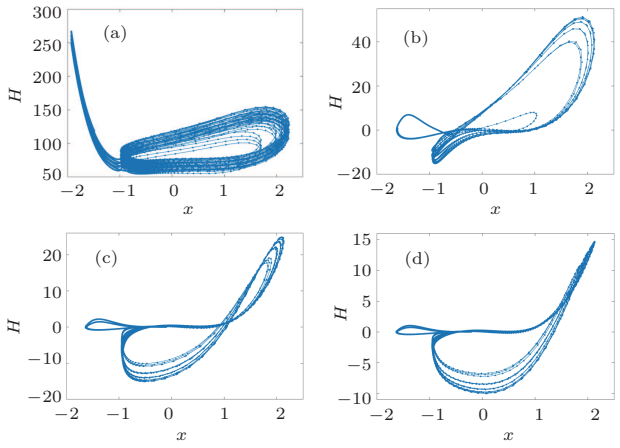


Fig. 9. The phase space of dynamics for periodic external forcing $I = I_1 + A\sin(0.05t)$, where $I_1 = 3.1$ and $A = 2.0$. The energy feedback is according to Eq. (12). (a) $k_4 = 0$, (b) $k_4 = 1.0$, (c) $k_4 = 5.0$, and (d) $k_4 = 10.0$.

The plots show that, as the feedback gain k_4 is increased the Hamilton energy function which is composed of the variables and bifurcation parameters controls the evolution of the system and the chaotic trajectories are stabilized. The variation of LLE is shown in Fig. 10. The maximum value of LLE is nearly equal to 0.008, greater than compared to the one obtained for constant external current.

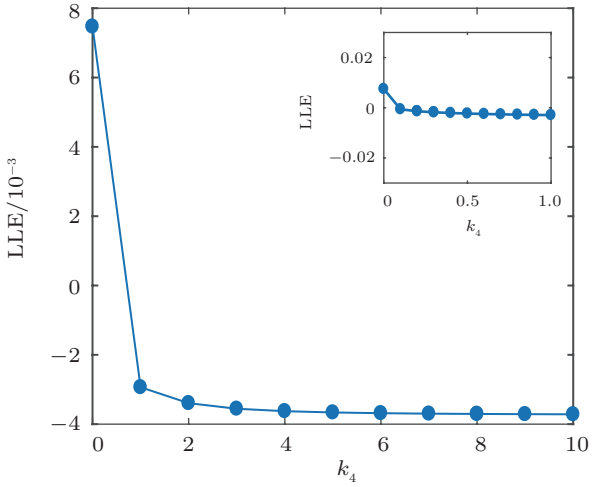


Fig. 10. Transition of LLE with k_4. Periodic variations are applied in the external current. The inserted figure is the enlarged version.

Case 3. White Gaussian noise

The phase portrait of the system with energy feedback in the presence of the external noise $I = I_1 + \zeta\xi(t)$ has also been studied with $I_1 = 3.1$ and $\zeta = 1$. As the feedback gain k_4 is increased, the noisy trajectories are controlled. Figures 11(a), 11(b), 11(c), and 11(d) represent the mechanism of the chaos control for $k_4 = 0$, $k_4 = 1.0$, $k_4 = 5.0$, and $k_4 = 10.0$ respectively. The LLE for noisy external forcing has the largest value in comparison with the previous cases as shown in Fig. 12. The increased Lyapunov exponent indicates sensitivity to initial conditions.

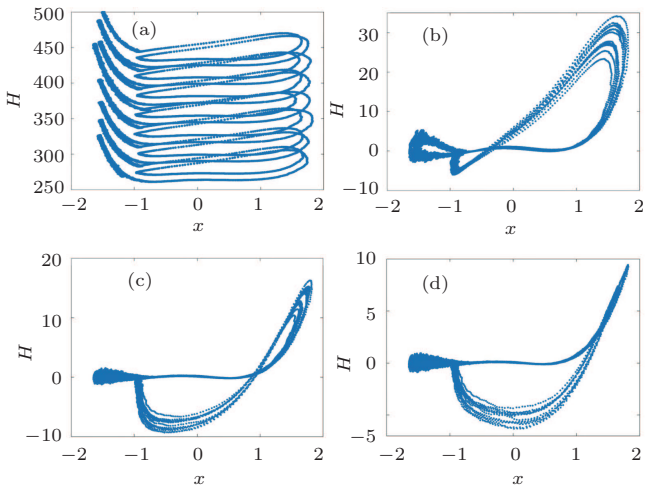


Fig. 11. Phase space in the presence of white Gaussian noise, ($I = 2 + \xi(t)$). The energy feedback obeys Eq. (12). (a) $k_4 = 0$, (b) $k_4 = 1.0$, (c) $k_4 = 5.0$, and (d) $k_4 = 10.0$.

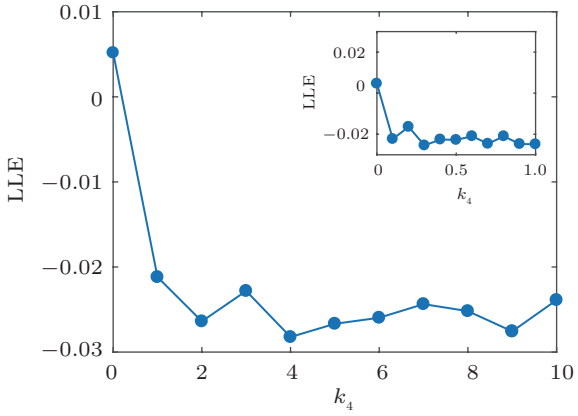


Fig. 12. Variations of LLE with k_4. White Gaussian noise is added as the external stimuli. The inserted figure is the enlarged version.

5. Synchronous dynamics

5.1. Electrical coupling

The dynamic equations for electrically coupled HR neuron model with quadratic flux controlled memristor has the form,

$$\begin{aligned}
\dot{x_1} &= y_1 + a{x_1}^2 - {x_1}^3 - z_1 + I - k_1\rho(\phi_1)x_1 - g_e(x_1 - x_2),\\
\dot{y_1} &= 1 - b{x_1}^2 - y_1,\\
\dot{z_1} &= r(R(x_1 - x_e) - z_1),\\
\dot{\phi_1} &= k_2 x_1 - k_3\phi_1 + D(\phi_1 - \phi_2), \qquad (13)\\
\dot{x_2} &= y_2 + a{x_2}^2 - {x_2}^3 - z_2 + I - k_1\rho(\phi_2)x_1 - g_e(x_2 - x_1),\\
\dot{y_2} &= 1 - b{x_2}^2 - y_2,\\
\dot{z_2} &= r(R(x_2 - x_e) - z_2),\\
\dot{\phi_2} &= k_2 x_2 - k_3\phi_2 + D(\phi_2 - \phi_1), \qquad (14)
\end{aligned}$$

where

$$\rho(\phi_i) = \alpha\phi_i^2 + \beta\phi_i + \gamma, \quad i = 1, 2.$$

The parameter g_e is the coupling strength of synaptic junction and D describes the field coupling strength. The parameters used are $a = 3.0$, $b = 5.0$, $R = 4.0$, $r = 0.006$, $x_e = -1.61$, $k_1 = 0.1$, $k_2 = 0.9$, and $k_3 = 0.5$, $\alpha = 0.4$, $\beta = 0.02$, and $\gamma = 0.1$.[9] We have evaluated the effect of modulation intensity of electromagnetic field in regulating the average energy of neurons in the synchronized state.

Figure 13(a) shows the average energy variations for $k_1 = 0.1$. The plot verifies that with increase in coupling strength the $\langle H \rangle$ changes in a waving pattern and it suddenly stabilizes at the point of synchronization. The membrane potential of both neurons are equal in the synchronized state and this leads to the vanishing of coupling term. As a result the energy in the synchronized state returns to its initial uncoupled value. Our results with quadratic flux controlled memristor are in accordance with the results obtained for HR model without memristor in Ref. [1]. The variation in $\langle H \rangle$ for an increased value of k_1 ($k_1 = 0.5$) is shown in Fig. 13(b). From the plot it is clear that as the value of k_1 is increased, the onset of synchronization occurs at a low value of g_e. The results imply that, an autonomous chaotic system with linear feedback coupling will move to its natural oscillatory regime in the synchronized state by gaining or dissipating energy. If the system continues in the same state, then the change in total average energy will be zero due to the repeating nature of trajectories with arbitrarily close energy values.

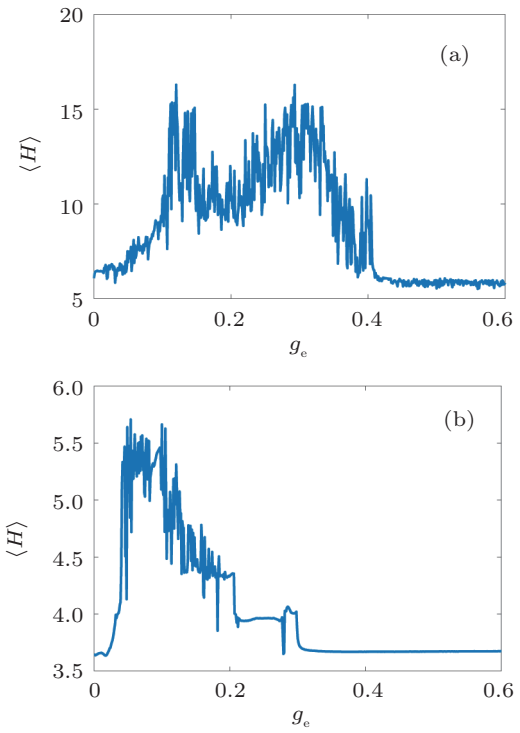


Fig. 13. Average energy of electrically coupled HR model by varying the coupling strength: (a) $k_1 = 0.1$ and (b) $k_1 = 0.5$.

The transition to the synchronized state is further confirmed by plotting the transverse Lyapunov exponents (TLE).[26] Figure 14(a) shows the variations of two of the largest TLEs with g_e for $k_1 = 0.1$. With increase in g_e, the largest TLE ($\lambda_{\perp_1}$) also starts to increase, reaches a maximum, and then starts to decrease. $\lambda_{\perp_1}$ crosses zero at $g_e = 0.41$ indicating a transition from desynchronized state to synchrony at this point.

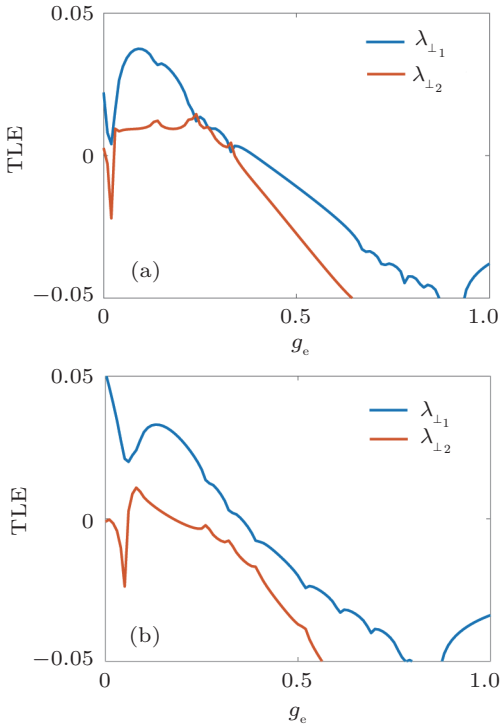


Fig. 14. TLEs of electrically coupled HR model by varying the coupling strength: (a) $k_1 = 0.1$ and (b) $k_1 = 0.5$.

Figure 14(b) shows the variations in TLEs for $k_1 = 0.5$. Here $\lambda_{\perp_1}$ crosses zero at a low value of g_e ($g_e = 0.37$). These results are consistent with the average energy changes shown in Fig. 13.

5.2. Chemical coupling

The equations governing the dynamics of chemically coupled HR neuron model with quadratic flux controlled memristor has the form,

$$\begin{aligned}
\dot{x_1} &= y_1 + a{x_1}^2 - {x_1}^3 - z_1 + I - k_1\rho(\phi_1)x_1 \\
&\quad - g_c(x_1 - V_s)/[1 + \exp(-\lambda(x_2 - \theta))], \\
\dot{y_1} &= 1 - b{x_1}^2 - y_1, \\
\dot{z_1} &= r(R(x_1 - x_e) - z_1), \\
\dot{\phi_1} &= k_2 x_1 - k_3\phi_1 + D(\phi_1 - \phi_2), \qquad (15) \\
\dot{x_2} &= y_2 + a{x_2}^2 - {x_2}^3 - z_2 + I - k_1\rho(\phi_2)x_1 \\
&\quad - g_c(x_2 - V_s)/[1 + \exp(-\lambda(x_1 - \theta))], \\
\dot{y_2} &= 1 - b{x_2}^2 - y_2, \\
\dot{z_2} &= r(R(x_2 - x_e) - z_2), \\
\dot{\phi_2} &= k_2 x_2 - k_3\phi_2 + D(\phi_2 - \phi_1), \qquad (16)
\end{aligned}$$

where

$$\rho(\phi_i) = \alpha\phi_i^2 + \beta\phi_i + \gamma, \quad i = 1, 2.$$

The parameter g_c is the coupling strength of synaptic junction and D describes the field coupling strength. V_s, the reversal potential is always greater than x for all neuron at all times. For each neuron to reach the threshold, we choose $\theta = -0.25$, $V_s = 2$, and $\lambda = 7.5$.[33]

The change in average energy with g_c for $k_1 = 0.1$ is shown in Fig. 15(a). From the plot it is clear that the fluctuating nature of average energy disappears at the point of synchronization. This occurs at $g_c = 1.55$. After that, the system shows an interesting behavior; *i.e.*, $\langle H \rangle$ linearly increases with increase in g_c.

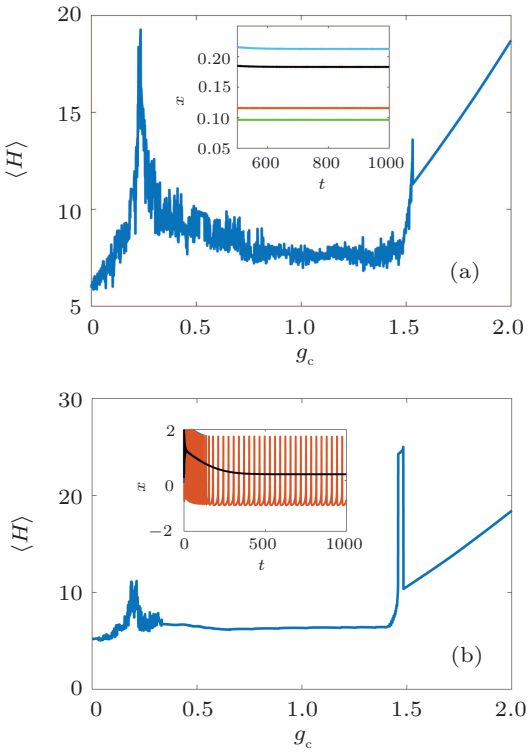


Fig. 15. Average energy of chemically coupled HR model by varying g_c for (a) $k_1 = 0.1$. The green, red, black, and blue lines in the inset plot shows the AD state obtained for $g_c = 1.55$, 1.7, 1.8, and 2, respectively. (b) Average energy variations for $k_1 = 0.2$. The inset plot represents the time series of membrane potential corresponding to periodically oscillating (red) and AD (black) states.

To unravel the reason for increase in $\langle H \rangle$ after $g_c = 1.55$, we have examined the time series of the system in the linearly increasing regime of $\langle H \rangle$. The results are shown in the inset plot of Fig. 15(a). The 'X' axis represents time and 'Y' axis denotes the membrane potential. The plot verifies that, even though both neurons are synchronized ($g_c \geq 1.55$), their membrane potential is in the amplitude death state (AD). The green, red, black and blue lines show the AD state which has been obtained for $g_c = 1.55$, 1.7, 1.8, and 2 respectively. As the value of g_c is increased the value of membrane potential at which AD takes place also increases. Thus, in chemical synaptic coupling where the interaction terms do not go to zero permits a change in average energy in the synchronized state. We have further analyzed the effect of k_1 in regulating $\langle H \rangle$. Figure 15(b) shows the $\langle H \rangle$ variations for $k_1 = 0.2$. For $0 < g_c \leq 0.55$, $\langle H \rangle$ shows some fluctuations and this region corresponds to the desynchronized state. After that, $\langle H \rangle$ remains constant for $0.55 < g_c \leq 1.484$ and linearly increases for $1.484 < g_c \leq 2.0$. The time evolution of membrane potential corresponds to these two cases are shown in the inset plot of Fig. 15(b). The periodically oscillating (red) time series is for the constant $\langle H \rangle$ regime, *i.e.*, in the synchronized state there occurs a transition to stable orbit and the total average energy change is zero due to the repeating nature of trajectories. The black line in the inset plot is the time evolution of membrane potential corresponding to the linearly increasing regime of $\langle H \rangle$. Here also AD occurs at different points for different values of g_c leading to a net average energy change. Thus it can be concluded that, an extra amount of energy is needed when a coupled system is forced to oscillate in different regions of the phase space where the average energy change is not zero. The extra demand of energy required for the collective dynamics is provided by the coupling mechanism.[34] In the central nervous system, some specialized structures are located at the postsynaptic sites for producing ATP molecules to balance the energy demands.[35]

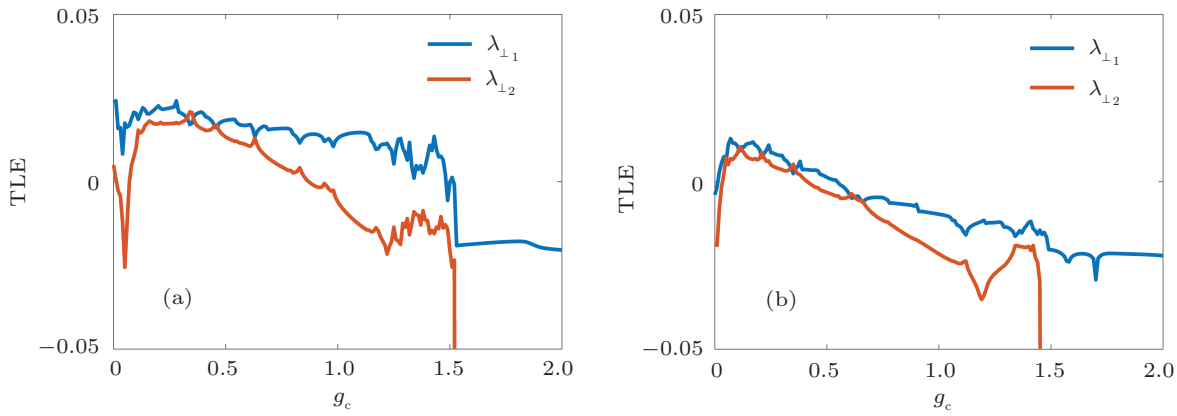


Fig. 16. TLEs of chemically coupled HR model by varying the coupling strength: (a) $k_1 = 0.1$ and (b) $k_1 = 0.2$.

The transition to the synchronized state is verified by plotting the TLEs. Figure 16(a) depicts the variations of two of the largest TLEs with chemical coupling strength for $k_1 = 0.1$. The $\lambda_{\perp_1}$ crosses zero at $g_c = 1.55$ corresponds to the synchronized state. For $k_1 = 0.2$, this transition occurs at a low value of g_c ($g_c = 0.55$), as shown in Fig. 16(b).

6. Results and conclusions

We have analyzed the energy aspects of single and coupled HR neuron models with a quadratic flux controlled memristor. The bifurcation analysis of single system by increasing the value of I suggest that the response of the system in the presence of external stimuli can be improved by properly modulating the electromagnetic induction. Based on Helmholtz theorem the rate of change of Hamilton energy of HR model with memristor has been derived. It is found that the average Hamilton energy decreases with increase in I. The time evolution of membrane potential and the rate of change of energy function for different external stimuli have been analyzed. In the case of constant external current, the electrical mode of neuron changes with the external forcing and energy is consumed for generating each action potential. In the presence of periodic stimuli, the firing mode changes with the change in amplitude of external forcing. The energy consumption of bursting state with less number of spikes per burst is found to be low compared to burst with more number of spikes. The analysis of the system by applying Gaussian white noise reveals that, bursting mode changes with increase in noise intensity. The bifurcation analysis corresponding to periodic input shows the presence of intermittently occurring states with the variations in A. The bifurcation diagram in the presence of noise reveals that as the noise intensity is increased, the system shows complex chaotic dynamics. The dependence of Hamilton energy function on system parameters is used to control and stabilize chaotic trajectories by giving a negative energy feedback. The suppression of chaotic trajectories and the stabilization of phase space of the system for periodic input and noise are discussed. As the feedback gain in the energy function is increased, the initially positive LLE become negative which in turn ensure the stabilization of chaotic trajectories.

In the case of electrically coupled neurons, as g_e is increased the $\langle H \rangle$ changes in a fluttering pattern and it stabilizes at the point of synchronization. The energy in the synchronized state returns to its initial uncoupled value due to the vanishing of coupling term in the synchronized state. This study has been repeated by increasing k_1 and found that for an increased value of k_1 the onset of synchronization occurs at a low value of g_e. The average energy variations exhibit three important regions when the neurons are coupled via chemical synapse. The fluctuating region indicates desynchrony. In the region where the $\langle H \rangle$ remains constant, the system shows synchronization with periodically oscillating dynamics and the total average energy change is zero due to the repeating nature of trajectories. In the linearly increasing regime, the dynamics are AD. As the value of g_c is increased, the value of membrane potential at which the system stabilizes is also increased and leads to a net average energy change. We conclude that if two neurons are coupled and forced to oscillate, then their phase space may contain different oscillatory regimes. As a result, the change in average energy of the system will not be zero and an additional amount of energy is used to sustain the synchronized state. The proposed method will be useful to study the energy aspects of other coupled chaotic and hyperchaotic systems. Possible extensions to neural networks can provide finer insight to the energy modulation mechanism of various biological systems.

Acknowledgments

UK would like to acknowledge University Grants Commission, India for providing financial assistance through JRF scheme for doing the research work. PAS would like to acknowledge DST, India for their financial assistance through the FIST program.

References

[1] Torrealdea F J, d'Anjou A, Grana M and Sarasola C 2006 *Phys. Rev. E* **74** 011905
[2] Torrealdea F J, Sarasola C and d'Anjou A 2009 *Chaos, Solitons and Fractals* **40** 60
[3] Sira-Ramirez H and Cruz-Hernandez C 2001 *Int. J. Bifur. Chaos* **11** 1381
[4] Sarasola C, Torrealdea F J, d'Anjou A, Moujahid A and Grana M 2004 *Phys. Rev. E* **69** 011606
[5] Moujahid A, d'Anjou A, Torrealdea F J and Torrealdea F 2011 *Chaos, Solitons and Fractals* **44** 929
[6] Moujahid A, d'Anjou A, Torrealdea F J and Torrealdea F 2011 *Phys. Rev. E* **83** 031912
[7] Gu H 2013 *Chaos* **23** 023126
[8] Pisarchik A N Jaimes-Reategui R and Garcia-Vellisca M A 2018 *Chaos* **28** 033605
[9] Xu Y, Ying H, Jia Y, Ma J and Hayat T 2017 *Sci. Rep.* **7** 43452
[10] Li H, Sun X and Xiao J 2018 *Chaos* **28** 043113
[11] Wang Y, Ma J, Xu Y, Wu F and Zhou P 2017 *Int. J. Bifur. Chaos* **27** 1750030
[12] Perc M and Marhl M 2006 *New J. Phys.* **8** 142
[13] Zambrano S, Marino I P, Seoane J M, Sanjuan M A F, Euzzor S, Geltrude A, Meucci R and Arecchi F T 2010 *New J. Phys.* **12** 053040
[14] Baltanas J P and Casado J M 2002 *Phys. Rev. E* **65** 041915
[15] Wang Y, Wang Z D and Wang W 2000 *J. Phys. Soc. Jpn.* **69** 276
[16] Lindner B, Garcia-Ojalvo J, Neimand A and Schimansky-Geiere L 2004 *Phys. Rep.* **392** 321
[17] Wu F, Wang C, Xu Y and Ma J 2016 *Sci. Rep.* **6** 28

[18] Wang G, Shen Y and Yin Q 2013 *Chin. Phys. B* **22** 050504
[19] Ma J, Zhou P, Ahmad B, Ren G and Wang C 2018 *PLOS ONE* **0191120** 1-21
[20] Ma J, Wu F, Jin W, Zhou P and Hayat T 2017 *Chaos* **27** 053108
[21] Xu F, Zhang J, Fang T, Huang S and Wang M 2018 *Nonlinear Dyn.* **92** 1395
[22] Thottil S K and Ignatius R P 2017 *Nonlinear Dyn.* **87** 1879
[23] Hindmarsh J L and Rose R M 1984 *Proc. R. Soc. Lond. B* **221** 87
[24] Rose R M and Hindmarsh J L 1985 *Proc. Roy. Soc. Lond. B* **225** 161
[25] Storace M, Linaro D and Enno de Lange 2008 *Chaos* **18** 033128
[26] Usha K, Subha P A and Chitra R N 2018 *Chaos, Solitons and Fractals* **108** 25
[27] Usha K and Subha P A 2018 *Int. J. Mod. Phys. C* **29** 1850023
[28] Guo Q, Gu W and Tao Z 2015 *Adv. Eng. Res.* 1461
[29] Lv M, Wang C, Ren G, Ma J and Song X 2016 *Nonlinear Dyn.* **85** 1479
[30] Juang J and Liang Y H 2015 *Chaos* **24** 013110
[31] Song X L, Jin W Y and Ma J 2015 *Chin. Phys. B* **24** 128710
[32] Djeundam S R D, Yamapi R, Kofane T C and Azizalaoui M A 2013 *Chaos* **23** 033125
[33] Somers D and Kopell N 1993 *Biol. Cybern.* **68** 393
[34] Wu K, Aoki C, Elste A, Rogalski-Wilk A A and Siekevitz P 1997 *Proc. Natl. Acad. Sci. USA* **94** 13273
[35] Siekevitz P 2004 *Science* **306** 410